Contents lists available at ScienceDirect

Virus Research

Exploring the enzymatic activity of depolymerase gp531 from *Klebsiella pneumoniae* jumbo phage RaK2

Algirdas Noreika [*], Jonita Stankevičiūtė, Rasa Rutkienė, Rolandas Meškys, Laura Kalinienė [*]

Department of Molecular Microbiology and Biotechnology, Institute of Biochemistry, Life Sciences Center, Vilnius, Lithuania

ARTICLE INFO

ABSTRACT

Klebsiella pneumoniae poses a major global challenge due to its virulence, multidrug resistance, and nosocomial nature. Thus, bacteriophage-derived proteins are extensively being investigated as a means to combat this bacterium. In this study, we explored the enzymatic specificity of depolymerase gp531, encoded by the jumbo bacteriophage vB_KleM_RaK2 (RaK2). We used two different methods to modify the reducing end of the oligosaccharides released during capsule hydrolysis with gp531. Subsequent acidic cleavage with TFA, followed by TLC and HPLC-MS analyses, revealed that RaK2 gp531 is a β-(1→4)-endoglucosidase. The enzyme specifically recognizes and cleaves the capsular polysaccharide (CPS) of the *Klebsiella pneumoniae* K54 serotype, releasing K-unit monomers (the main product), dimers, and trimers. Depolymerase gp531 remains active from 10 to 50 °C and in the pH 3–8 range, indicating its stability and versatility. Additionally, we demonstrated that gp531′s activity is not affected by CPS acetylation, which is influenced by the growth conditions of the bacterial culture. Overall, our findings provide valuable insights into the enzymatic activity of the first characterized depolymerase targeting the capsule of the clinically relevant K54 serotype of *K. pneumoniae*.

1. Introduction

Bacteria of the genus *Klebsiella* are widely distributed in nature and can be found in diverse environments, including soil, water, plants, as well as the gastrointestinal tract and nasopharynx of animals and humans (Podschun and Ullmann, 1998; Patro and Rathinavelan, 2019). While generally harmless to people with a healthy immune system, certain species of *Klebsiella* are increasingly being linked to healthcare-associated as well as community-acquired infections (Patro and Rathinavelan, 2019; Effah et al., 2020; Rocha et al., 2022). Among these species, the opportunistic pathogen *Klebsiella pneumoniae* is considered the most clinically relevant, causing up to one-third of nosocomial Gram-negative bacterial infections worldwide (Navon-Venezia et al., 2017; Rocha et al., 2022). The emergence and rapid spread of drug-resistant (DR) and hypervirulent DR strains of *K. pneumoniae* have contributed significantly to the increasing morbidity and mortality associated with these infections (Russo and Marr, 2019; Zhu et al., 2021; Shao et al., 2022; Taha et al., 2023).

The major virulence factors that contribute to the pathogenicity of *K. pneumoniae* are the capsular polysaccharide (CPS, commonly referred to as K-antigen), the O-side-chain of lipopolysaccharide (O-antigen),

adhesins, and iron uptake systems (Zhu et al., 2021; Riwu et al., 2022). The capsule, a dense polysaccharide layer that completely covers the surface of the bacterium, is widely recognized as a key determinant of virulence (Patro and Rathinavelan, 2019; Wu et al., 2023). The capsule offers several advantages in the infection process. First, it provides protection against host immune responses, making it difficult for the immune system to recognize and eliminate the bacterium (Hager et al., 2019; Bellich et al., 2020). Second, the capsule facilitates the adhesion of the bacteria to host mucous membranes, promoting colonization and the establishment of the infection (Wilson, 2002; Huynh et al., 2017; Chen et al., 2023). The *K. pneumoniae* capsule, composed of linear or branching repeating oligosaccharide units that may contain up to seven monosaccharides (such as D-glucose, D-galactose, D-mannose, L-rhamnose, L-fucose, etc.) linked by glycosidic bonds, exhibits remarkable structural diversity in terms of sugar composition, linkage types and patterns, and the specific ratio of noncarbohydrate substituents (Zamze et al., 2002; Pan et al., 2015; Patro and Rathinavelan, 2019; Bellich et al., 2019; 2020; Knirel and Van Calsteren, 2021). To date, more than 70 distinct *K. pneumoniae* capsule variants (K-types or K-serotypes) have been described by serological methods and/or genotyping, with their polysaccharide structures determined (Opoku-Temeng et al., 2019;

---

* Corresponding authors.
E-mail addresses: algirdas.noreika@gmc.vu.lt (A. Noreika), laura.kaliniene@bchi.vu.lt (L. Kalinienė).

Patro and Rathinavelan, 2019; Bellich et al., 2020). Among these variants, K1, K2, K5, K20, K54, and K57 are the most commonly found in hypervirulent strains of *K. pneumoniae*, which are increasingly associated with community-acquired invasive pyogenic liver abscesses, sepsis, and pneumonia (Riwu et al., 2022; Taha et al., 2023; Wu et al., 2023). As mentioned above, such hypervirulent strains often carry diverse antimicrobial resistance genes, necessitating the development of alternative treatments to antibiotic therapy. In this regard, phage-borne enzymes specifically targeting the bacterial capsule provide a promising avenue for combating *K. pneumoniae* infections. In fact, several studies have shown that decapsulation of *K. pneumoniae* cells using, for example, recombinant phage depolymerases increases the susceptibility of the bacteria to serum-mediated killing (Lin et al., 2014; Majkowska-Skrobek et al., 2016; 2018; Wang et al., 2019; Volozhantsev et al., 2020; Wu et al., 2023).

In *K. pneumoniae*-infecting viruses, CPS-degrading depolymerases are usually virion-associated and function as the enzymatic receptor-binding proteins (RBPs). Such RBPs specifically recognize and then cleave the cellular capsule to allow the virus particle to reach its secondary receptors, typically located on the outer membrane (Bertozzi Silva et al., 2016; Fernandes and São-José, 2018; Knecht et al., 2020; Knirel et al., 2020; Noreika et al., 2023). Just like other phage depolymerases, which target LPS or exopolysaccharides, K-type specific enzymes encoded by *K. pneumoniae* bacteriophages are classified as lyases or hydrolases (Squeglia et al., 2020). Lyases directly act on their substrate, utilizing it as a proton donor, and cleave the glycosidic bond via β-elimination, resulting in the formation of unsaturated (oligo)saccharides. Hydrolases, on the other hand, use a water molecule to break the bond, resulting in saccharides with a restored hydroxyl group (Jongkees and Withers, 2014; Olszak et al., 2017; Stone et al., 2008). Interestingly, most of the data on the mechanisms of the enzymatic reactions carried out by *Klebsiella* phage depolymerases were gathered decades ago in studies aimed at determining or refining the structure of CPS of different K-serotypes (e.g., K2 (Sutherland, 1971), K3 (Dutton et al., 1986), K13 (Niemann et al., 1977), K15 (Parolis et al., 1992), K25 (Thurow et al., 1974), K54 (Dutton and Merrifield, 1982; Sutherland, 1967; Sutherland and Wilkinson, 1968), etc.). The results of these pioneering studies of that time showed that most of the CPS depolymerases produced by *K. pneumoniae* phages are glycoside hydrolases (i.e., mannosidases, fucosidases, galactosidases, glucosidases, etc.), which predominantly cleave the β-(1→3) or β-(1→4) glycosidic bonds. Unfortunately, in most cases no detailed information is available on the phages used, their genomes, or the specific phage proteins responsible for CPS degradation.

Since then, *K. pneumoniae* phages targeting capsular types such as K1 (e.g. phage phiK64-1; Pan et al., 2017), K2 (phage B1; Pertics et al., 2021), K3 (phage KP32; Squeglia et al., 2020), K5 (phage K5-4), K8 (Hsieh et al., 2017), K20 (phage vB_KpnM-20; Wu et al., 2023), K57 (phage vB_KpnP_ZX1; Li et al., 2022), among others, have been isolated. Their corresponding CPS depolymerases have been identified and functionally characterized. Nevertheless, to the best of our knowledge, no genetically as well as biochemically characterized depolymerases capable of degrading the CPS of *K. pneumoniae* K54 may be found in the literature. Furthermore, despite the large number of identified *K. pneumoniae* phage depolymerases, only a few of these enzymes, such as the β-(1→3)-endogalactoside hydrolases, Dep_kpv79 and Dep_kpv767 (Volozhantsev et al., 2020), and the phage NTUH-K2044-K1-1 lyase, gp34 (Tu et al., 2022), have been thoroughly investigated in terms of their specific enzymatic activity. In addition, a depolymerase encoded by the *K. pneumoniae* phage RAD2 has been shown to cleave the K2 capsule by releasing dimers and trimers of the structural K-unit, suggesting that this enzyme is an endoglycosidase. However, the precise glycosidic bond targeted by RAD2 depolymerase has not been identified (Dunstan et al., 2021).

In our previous study on the adsorption complex of alcyoneusviruses, we investigated the biological function of gp531, a depolymerase domain-containing protein encoded by the unique *Klebsiella* jumbo phage RaK2 (Noreika et al., 2023). Our findings revealed that RaK2 gp531 is a component the long tail fiber and functions as a homotrimer and is essential for the recognizing and attaching to *K. pneumoniae* KV-3 cells.

Here, we explored the enzymatic properties of RaK2 gp531. We established that gp531 is a β-(1→4)-endoglucosidase that cleaves the K54-type CPS. We also observed that the level of CPS acetylation, influenced by the growth conditions of the bacterial culture, had no effect on the enzymatic activity of this protein. Additionally, we demonstrated that gp531 retains its activity within a pH range of 3 to 8 and at temperatures ranging from 10 to 60 °C. Overall, these findings significantly contribute to our understanding of how phage-encoded RBPs target the capsule of *K. pneumoniae*. Moreover, they provide valuable insights into the enzymatic activity of RaK2 gp531, the first characterized depolymerase targeting the CPS of the clinically relevant K54 serotype of *K. pneumoniae*.

2. Materials and methods

2.1. Klebsiella sp. KV-3 genotyping

To determine the K-type of *Klebsiella* sp. KV-3, a bioinformatic analysis was performed on a 30.887 bp genome fragment (3637592… 3668479) of the bacterium. This region encompasses the *cps* cluster, flanked by *terC* and *rfbA* at the 5′ and 3′ termini, respectively. Open-source tools such as BlastN and MultiGeneBlast (https://multigenebl ast.sourceforge.net) were utilized for the analysis using default parameters. To aid in the identification process, we utilized a reference database of 81 *Klebsiella* K-serotypes with known polysaccharide structures and *cps* genotypes (Table S1). Additionally, two open-source tools, namely K-Pam (Patro et al., 2020) and Kaptive (Wick et al., 2018), were used to verify the serotype prediction.

2.2. Recombinant RaK2 gp531

The isolation of bacteriophage RaK2, *K. pneumoniae* KV-3 propagation, as well as the construction and purification of recombinant gp531 were performed according to previously described methods (Noreika et al., 2023; Šimoliunas et al., 2013).

Briefly, to obtain the recombinant RaK2 gp531, the appropriate gene was amplified using specific forward (5′-CTT GTC GAC GAG GTT TAA TAT GTC ATT GA-3′) and reverse (5′-TAG GAT CCT TTT TTA TAC TGA AGT TCC TG-3′) primers. The resulting amplicon was then inserted into the expression vector pET16b, and the constructed plasmid was transformed into *Escherichia coli* Rosetta (DE-3). Following induction with IPTG (0.5 mM), a recombinant 100-kDa protein with a His × 10 tag at the N-terminus was produced and was purified by Ni-NTA chromatography.

2.3. K. penumoniae KV-3 CPSs isolation

To facilitate CPS production, an overnight culture of *K. pneumoniae* KV-3 (10 mL) was transferred to a flask with 200 mL Luria Broth (LB) and incubated at 37 °C for 11 days without agitation. CPS isolation procedure followed a previously described method with minor adjustments (Bales et al., 2013). Briefly, 1.2 mL of a 37 % formaldehyde solution (Fluka AG, Germany) was added to 200 mL of the bacterial culture. The sample was then incubated with gentle agitation at 22 °C for an hour. Subsequently, 100 mL of 1 M NaOH was added, and the sample was further incubated with increased agitation for 3 h. The resulting supernatant, containing the CPSs, was collected by centrifugation (10,000 rpm, 4 °C, 1 h) and then concentrated using an ultrafiltration membrane (10 kDa cut-off; Pall Corporation, USA) to reduce the volume to one-tenth of the original. The sample was then dialyzed against Milli-Q water and treated with trichloroacetic acid (20 % w/v; British Drug Houses Chemicals, England) to precipitate impurities, such

as proteins and nucleic acids. After centrifugation at 10,000 rpm and 4 °C for one hour, a precipitate-free supernatant was collected, mixed with cold ethanol (final concentration of 58–60 %), and the CPS was precipitated for 16 h at −20 °C. The CPS was then pelleted by centrifugation (10,000 rpm, 4 °C, 1 h), dissolved in Milli-Q water, transferred to a dialysis tube (30-kDa cut-off) and dialyzed against Milli-Q water. Finally, the isolated CPS was lyophilized to a cotton-like substance.

2.4. Isolated and wild type CPSs hydrolysis with gp531

To explore the depolymerase activity of gp531, isolated CPSs of *K. pneumoniae* KV-3 were used as a substrate. The enzymatic reaction was carried out at 30 °C in a 20 mM sodium phosphate solution (pH 6.0) for 0.5–20 h, using different amounts of the isolated CPS (0.15–12 mg) and gp531 (0.3–25 μg). To inactivate the enzyme, acetonitrile (ACN; Sigma-Aldrich, USA) was added in a 1:1 volume ratio. After a brief centrifugation (10,000 rpm, 8 min), the resulting insoluble precipitate was removed, and the supernatant was analyzed by thin-layer chromatography (TLC) and high-performance liquid chromatography–mass spectrometry (HPLC-MS). Enzymatic hydrolysis of the CPS of whole cells was performed following the procedure described previously (Noreika et al., 2023).

2.5. TLC analysis

The samples were spotted (1–2 μL) onto TLC Silica Gel 60 F_{254} plates (Merck, Germany). A TLC mobile phase of 1-propanol (1-proOH; Merck, Germany), ethyl acetate (EtOAc; Honeywell, Riedel-de Haen, Germany), and deionized water (dH$_2$O) in a volume ratio of 6:1:3 was used to separate mono- and disaccharides, whereas a mobile phase of 1-butanol (1-butOH; Merck, Germany), ethanol (EtOH), and dH$_2$O in a volume ratio of 5:3:2 was used for the separation of tetra- and higher saccharides.

The plates were then dried and stained using a 1 % of 4-anisaldehyde (Sigma-Aldrich, Germany) prepared in a solution containing 90 % ethanol, 1 % acetic acid (Lach-Ner, Czech Republic), and 3.6 % sulfuric acid (Lach-Ner, Czech Republic). After drying, the plates were gently heated until the separated compounds became visible. For the saccharides derivatized with 8-aminonaphthalene-1,3,6-trisulfonic acid (ANTS, Sigma-Aldrich, Switzerland), a 365-nm wavelength light was used to detect the separated compounds. The colors of the images were inverted to improve the visibility of the separated compounds.

TLC was routinely run for 20–25 min and repeated up to three times to ensure better separation of compounds.

2.6. HPLC-MS analysis

CPS hydrolysis samples, commercially acquired mono- and disaccharides, and their chemically modified compounds, were analyzed using the HPLC-MS system (Shimadzu, Japan) equipped with a photodiode array detector (Shimadzu, Japan) and a mass spectrometer (LCMS-2020; Shimadzu, Japan) with an electrospray ionization source. Chromatographic separation was carried out on a *YMC-Pack Pro*-C18 column (3 × 150; YMC, Japan) at 40 °C. Two different mobile phases were used: 0.1 % formic acid (HCOOH) water solution (solvent A) with acetonitrile (ACN, solvent B), or a 10 mM ammonium carbonate ((NH$_4$)$_2$CO$_3$) water solution with ACN. The gradient elution mode was employed with a 5–95 % gradient over a 12-min period. Mass scans were measured in the 250–2000 m/z range at a 350 °C interface temperature, 250 °C desolvation line temperature, ±4500 V interface voltage, and neutral DL/Qarray, using N$_2$ as the nebulizing and drying gas. Mass spectrometry data were acquired in both positive and negative ionization modes and analyzed using *LabSolutions* liquid chromatography-mass spectrometry software.

2.7. Depolymerase substrate screening

To investigate the substrate specificity of gp531, a screening of various compounds (Table S3) was performed. For the first set of reactions, 1 mM of the chromogenic compound and 1 μg of gp531 were mixed in a 100 μL total volume of 50 mM Tris buffer solution (pH 8). The enzymatic reaction was conducted at 30 °C for 1–2 h, and the resulting yield was measured using a spectrophotometer.

The second set of reactions consisted of 2 mM of saccharides or 3 mg/mL of polysaccharides and 3 μg of gp531, in a total volume of 20 μL in 20 mM sodium phosphate solution (pH 6). After 16–18 h of reaction at 37 °C, the samples were analyzed using the TLC assay.

2.8. Saccharide reduction with NaBH$_4$

To modify the reducing end of the products obtained after CPS (0.6 mg) hydrolysis with gp531, a reduction reaction was performed in a solution containing 0.15 M sodium borohydride (NaBH$_4$; Sigma-Aldrich, USA) and 2.5 mM KOH with a total volume of 200 μL, at 20–25 °C for 24 h in the dark. To neutralize the excess reagent, 15 % of the sample volume of a 2 M acetic acid solution was added. Controls, including L-fucopyranose (L-Fuc*p*; Carbosynth, United Kingdom), D-glucopyranose (D-Glc*p*; Alfa Aesar, USA), D-glucopyranuronic acid (D-Glc*p*A; Sigma-Aldrich, USA), and D-cellobiose (D-Cell; Honeywell Fluka Analytical, USA), were reduced using a three-fold molar quantity of NaBH$_4$. Subsequently, all the samples were dried in a vacuum concentrator, reconstituted in water, and analyzed by TLC and HPLC-MS.

2.9. Saccharide derivatization with ANTS

To modify the reducing end of the products obtained after CPS (12 mg) hydrolysis with gp531, a derivatization reaction with ANTS was performed. For this, 0.2 M ANTS dissolved in 2.62 M acetic acid and 1 M sodium cyanoborohydride (NaCNBH$_3$; Sigma-Aldrich, USA) prepared in DMSO were mixed in a 1:1 ratio and the resulting buffer solution was poured over the dried product sample, resulting in a total volume of 250 μL. The reaction was carried out for 24 h at 37 °C. Afterward, the sample was concentrated using a vacuum concentrator, and the ANTS-derivatized product from CPS hydrolysis was purified by a fast protein liquid chromatography (FPLC) technique. The control saccharides (L-Fuc*p*, D-Glc*p*, D-Glc*p*A, and D-Cell) were also derivatized using a molar ratio of 6:5:25 (saccharide: ANTS: NaCNBH$_3$).

2.10. ANTS-derivatized tetrasaccharide purification

To remove the excess fluorophore from the ANTS-derivatized tetrasaccharide, the main product of CPS hydrolysis with gp531, it was purified using the *General Electric (GE) Akta Purifier 100* FPLC system. Initial purification was performed on a 1-mL *Hitrap* ion-exchange column DEAE FF (GE Healthcare, Sweden) using two solutions: Solution A (20 mM sodium phosphate, pH 8.1, and 3 mS/cm) and Solution B (20 mM sodium phosphate, 1.0 M NaCl, pH 8.1, and 72 mS/cm). The sample was fractionated into 0.5 mL aliquots in the following steps: 0–50 % gradient of B, 8.2 column volumes (CVs); 50 % B, 18.5 CVs; 50–100 % B, 8 CVs; and 100 % B, 15 CVs. The signal of ANTS derivatives was measured at a wavelength of 365 nm, and fractions without ANTS were identified by TLC. The ANTS-free fractions were combined, vacuum-dried, and subjected to gel filtration on a 370 × 10 mm column, manually loaded with 30 mL of *Sephadex SG-10* resin (Pharmacia Fine Chemicals, Sweden). The column was washed with deionized water (3 CVs), and a sample volume corresponding to 3 % of the column's volume was injected. The eluted fractions of 0.5 mL were collected and analyzed by TLC.

2.11. TFA acid hydrolysis

To identify the reducing end sugar residue of polysaccharide hydrolysis products generated by the gp531-catalyzed reaction, these products and the compounds formed during their reactions with NaBH₄ or ANTS as well as ANTS-cellobiose were hydrolyzed with 4.0 M tri-fluoroacetic (TFA; Sigma-Aldrich, Germany) acid at 90 °C for 10–180 min. Then, the resulting hydrolysates were dried using a vacuum concentrator, reconstituted in water, and analyzed by TLC and HPLC-MS.

2.12. Temperature and pH influence on the enzymatic activity of gp531

To investigate the effect of temperature and pH on the enzymatic activity of RaK2 depolymerase 531, purified recombinant protein and its substrate, isolated *K. pneumoniae* KV-3 CPS, were used. To evaluate the effect of temperature, reaction mixtures containing 20 μL of 20 mM sodium phosphate buffer solution (pH 6.0), 45 μg of CPS and 0.3 μg of gp531 were prepared. After 90 min at 10–70 °C, the reaction mixtures were diluted with an equal volume of ACN, centrifuged (8 min, 10,000 rpm, 22 °C), and the resulting supernatants analyzed by HPLC-MS. As a control sample, a reaction mixture was prepared at 20 °C and inactivated with ACN (1:1) after the other samples had reached the appropriate measuring temperatures.

To assess the influence of pH, the reactions were carried out in the pH range of 3–10. The reaction mixtures consisted of 25 μL of the appropriate buffer solution (50 mM citrate, pH 3–6; 50 mM Tris, pH 7–9; or 50 mM sodium borate, pH 10), together with 75 μg of CPS and 1 μg of gp531. A protein-free reaction mixture, prepared in 50 mM citrate at pH 3 was used as a control. After 16 h at 22 °C, the mixtures were diluted with an equal volume of ACN, centrifuged (8 min, 10,000 rpm, 22 °C), and the resulting supernatants were analyzed by HPLC-MS. The enzymatic activity was quantified by integrating the total area of the ion peaks at m/z 663 and 687 within a 2–4 min range and subtracting the values of the control samples to calculate the relative activity.

3. Results

3.1. K-typing of K. pneumoniae KV-3

Analysis of the *K. pneumoniae* KV-3 capsular polysaccharide synthesis gene region (*cps*) using MultiGeneBlast revealed that it has the highest degree of homology (99–100 % sequence identity between homologous proteins) with *K. pneumoniae* K54 serotype *cps* region. The second and third closest homologs were *K. pneumoniae* K16 (61–100 %) and K1 (50–99 %). However, additional glycosyl/acetyltransferase genes are found in the K16 *cps* region while the Wzx and Wzy proteins of K16 show no homology to those of K54 (Fig. 1).

K-typing of KV-3 was also performed using K-Pam (Patro et al., 2020) and Kaptive (Wick et al., 2018), both of which yielded results consistent with the findings obtained from the MultiGeneBlast analysis. These combined results provided strong evidence that *K. pneumoniae* KV-3 belongs to the capsular type K54.

3.2. Cleavage of K. pneumoniae KV-3 CPS with gp531

According to the literature, the repeating K-unit of K54 CPS is a branched tetrasaccharide (Fig. 2A) with a polysaccharide main chain of →4)-α-D-Glc*p*A-(1→3)-α-L-Fuc*p*2Ac-(1→3)-β-D-Glc*p*-(1→ and a single β-(1→4) linked side-chain residue (β-D-Glc*p*). Also, as shown in Fig. 2A, every second K54 K-unit is acetylated (Dutton and Merrifield, 1982; Dell et al., 1983).To investigate how RaK2 gp531 cleaves the capsule of KV-3, the recombinant protein was incubated with the purified CPS of KV-3 as a substrate, and the resulting oligosaccharide products were then analyzed by TLC and HPLC-MS.

TLC analysis (Fig. 2B) revealed that products of varying sizes are generated upon KV-3 CPS cleavage with gp531, and that the main reaction product (band 2 on the TLC plate) likely contains only a few sugar residues. This finding was further supported by HPLC-MS analysis, which demonstrated that depolymerization of KV-3 CPS with gp531 leads to the formation of three main reaction products, i.e., oligosaccharides M_I, M_{II}, and M_{III} (Fig. 2C). The mass spectra of these products showed [M-H]⁻ ion peaks at m/z 663, 1309, and 1955, respectively, and were in good agreement with the theoretical m/z values calculated for the K54 CPS hydrolysis products, namely the monomer (tetra-saccharide), dimer (octasaccharide), and trimer (dodecasaccharide) of the K-unit (Table S2). Based on the results of HPLC-MS, a tetrasaccharide is the main product of CPS hydrolysis with gp531, as indicated by the prominent [M-H]⁻ ion peak at m/z 663. Interestingly, however, we detected no signals at the masses expected for acetylated compounds (Table S2).

As mentioned above, at least two independent studies have shown that K54 CPS is O-acetylated, although this modification is rather non-stoichiometric, as is typical of most *K. pneumoniae* capsular serotypes (Dutton and Merrifield, 1982; Dell et al., 1983; Knirel and Van Cal-steren, 2021). In addition, the O-acetyltransferase gene, *wckB*, is intact at the *cps* locus of *K. pneumoniae* KV-3 (Fig. 1), suggesting that its capsular polysaccharide should be acetylated. On the one hand, it is possible that O-acetyl groups are lost during the purification process of CPS (Ucieklak et al., 2017). On the other hand, it has been previously shown that the O-acetylation of capsular polysaccharides varies between different strains of the same K-type (Hsu et al., 2016) and that the presence of an acetyltransferase gene at the *cps* locus does not guarantee the presence of this modification in the CPS of a particular strain (Pan et al., 2014). Taking all this into account, we decided to further investigate the acetylation phenomenon of the KV-3 capsule by repeating the HPLC-MS analysis described above with a slight modification: instead of using purified CPS as a substrate for gp531, we used a *K. pneumoniae* KV-3 cell culture (Fig. 3). Simultaneously, we aimed to explore the potential impact of this modification on the function of gp531, considering previous reports suggesting that fine variations in the CPS structure promote resistance to phage depolymerases (Venturini et al., 2020).

HPLC-MS analysis revealed that incubation of gp531 with a fresh biomass of KV-3 (2 h of cultivation at 37 °C, 190 rpm, OD_{600} 2.5), resulted in the formation of two main hydrolysis products of CPS, an acetylated tetrasaccharide and a diacetylated octasaccharide (corresponding [M-H]⁻ ion peaks at m/z 705 and 1393, respectively) (Fig. 3A). However, when the culture was allowed to grow for two days in liquid medium without agitation, a decrease in the acetylation extent of KV-3 CPS was observed, as no signals at the masses expected for a diacetylated
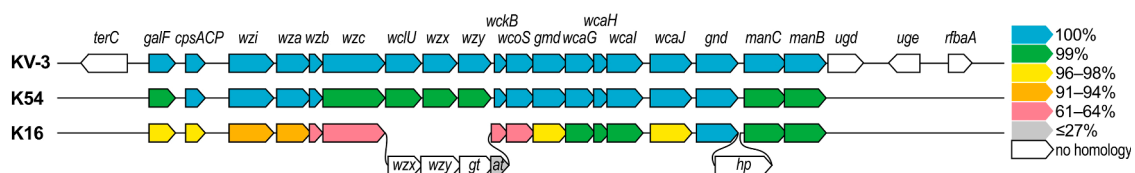

Fig. 1. Comparison of *cps* gene regions among K54, K16, and *K. pneumoniae* KV-3. Open reading frames are shown as arrows colored according to homology. The color code is shown on the right side of the image. Gt – glycosyltransferase, at – acetyltransferase, hp – hypothetical protein.
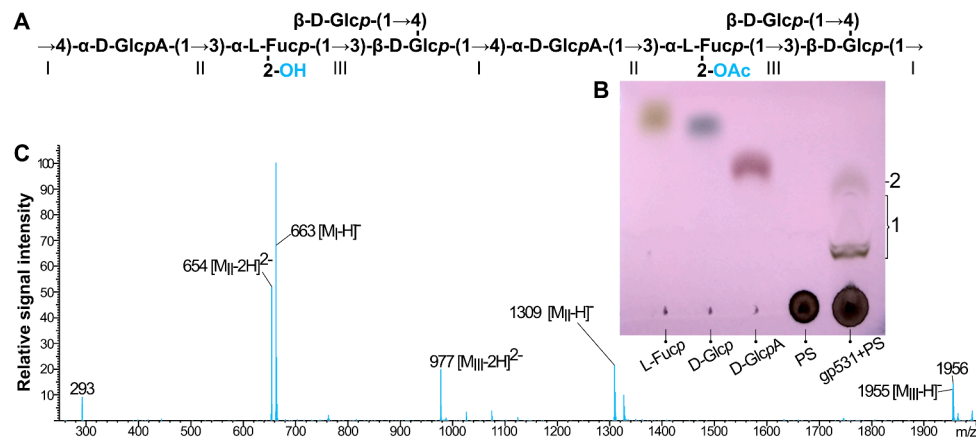
Fig. 2. TLC and HPLC-MS analysis of the reaction products from the cleavage of *K. pneumoniae* KV-3 CPS with RaK2 gp531. (A) Structure of *Klebsiella pneumoniae* K54 CPS is depicted as a dimer of the K-unit (Dell et al., 1983; Dutton and Merrifield, 1982). Roman numerals indicate different backbone glycosidic bonds. The acetylation site is marked in blue; (B) TLC analysis of gp531-treated KV-3 CPS. TLC was performed using a mobile phase composed of 1-propanol (1-proOH), ethyl acetate (EtOAc), and deionized water (dH₂O) mixed in a ratio of 6:1:3. The total run time for the analysis was 20 min. The bands on the TLC plate represent octasaccharide and higher oligosaccharides (1), and the final reaction product, potentially tetrasaccharide (2); (C) Negative-mode mass spectra of gp531-treated KV-3 CPS analyzed by HPLC-MS.
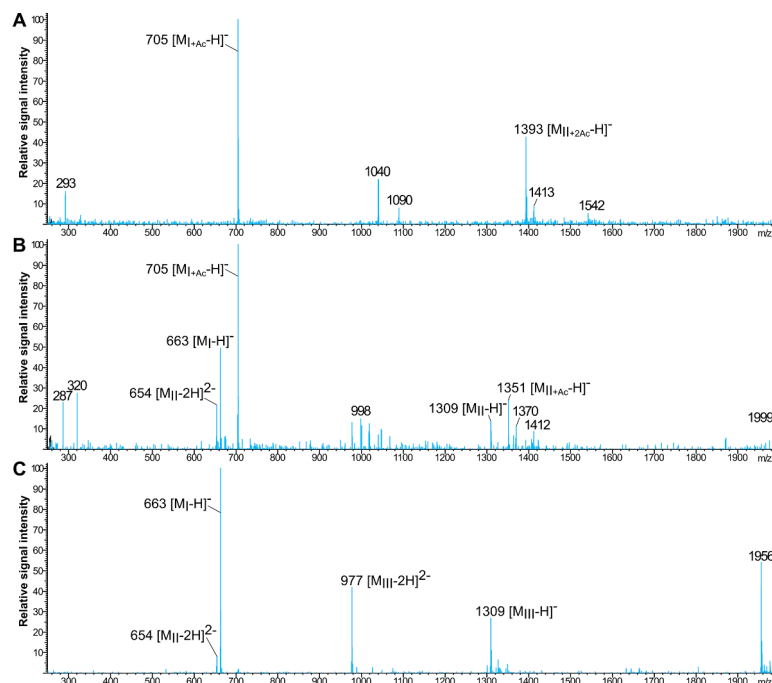

Fig. 3. Negative-mode mass spectra of products obtained after treatment of *K. pneumoniae* KV-3 cells with gp531. Cells were grown at 37 °C for 2 h with continuous agitation at 190 rpm (A), 2 (B) and 11 days without agitation (C).

octasaccharide were detected in the mass spectra of the gp531-mediated hydrolysis products (Fig. 3B). Instead, in the negative-ion mode, a monoacetylated octasaccharide (m/z 1351, [M-H]⁻) and an acetylated tetrasaccharide (m/z 705, [M-H]⁻) were detected and identified along with the unmodified tetra- (m/z 663, [M-H]⁻) and octasaccharides (m/z 1309, [M-H]⁻).

Finally, as depicted in Fig. 3C, the mass spectra of the reaction products obtained from the gp531-treated cells showed no prominent peaks corresponding to acetylated compounds suggesting that after 11 days of cultivation, the KV-3 CPS is either completely deacetylated or only marginally acetylated. This result clearly explains why only deacetylated compounds were detected in our initial studies. As described in the Materials and Methods section, the substrate for gp531 in these experiments was CPS isolated from an 11-day culture of KV-3

cells.

In summary, the results of the above studies reveal that: (i) gp531 is the K54 serotype-specific depolymerase, which cleaves the CPS of *K. pneumoniae* KV-3 by the hydrolytic mechanism; (ii) variations in CPS acetylation have no effect on gp531 hydrolytic activity, and (iii) in *K. pneumoniae* KV-3, the extent of CPS acetylation depends on the growth conditions of the bacteria. However, the question remains as to which specific glycosidic linkage is hydrolyzed by RaK2 gp531.

3.3. Identification of the specific glycosidic linkage cleaved with gp531

Based on their mode of action, glycosidases are classified into two main types: endoglycosidases and exoglycosidases. Exoglycosidases specifically target and remove the terminal monosaccharide residue

from the non-reducing end of sugar chains. In contrast, endoglycosidases cleave the inner part of sugar chains, releasing oligosaccharides (Kobata, 2013).

The results of the studies described in the previous section showed that gp531 is definitely an endoglycosidase. However, the specific glycosidic linkage that the enzyme cleaves could not be determined based on those results. Thus, a wide range of commercial chromogenic derivatives, as well as oligo- and polysaccharides (Table S3) were employed as substrates for RaK2 gp531. The test revealed that gp531 does not hydrolyze any of the 27 substrates tested, suggesting that the specificity of gp531 is directed towards a fragment of the sugar chain rather than a specific glycosidic linkage.

According to the results of the HPLC-MS analysis described in the previous section, the main product resulting from the cleavage of *K. pneumoniae* type K54 CPS with gp531 is a tetrasaccharide. As shown in Fig. 1, the backbone of the K54 K-unit contains fucose, glucose, and glucuronic acid residues linked together by the β-(1→4) and α-(1→3) glycosidic linkages. Thus, depending on which glycosidic bond is cleaved, enzymatic degradation of KV-3 CPS with gp531 can produce one of three possible tetrasaccharides, each with the same molecular mass but a different structure. Taking advantage of this feature, we applied a reducing end modification technique to determine the structure of the oligosaccharide produced by gp531 and to identify the glycosidic linkage targeted by the enzyme.

First, the hydrolysate of K54 CPS, produced by gp531, was modified through a reduction reaction using NaBH₄. Subsequently, both the unreduced and reduced samples were cleaved with 4 M TFA acid (Fig. 4A) to obtain smaller saccharide units. Commercial monosaccharides L-Fuc*p*, D-Glc*p*, D-Glc*p*A, and D-Cell, were also subjected to

reduction by NaBH₄ and, together with their unreduced counterparts, were used as controls (Fig. 4B).

The results of TLC analysis (Fig. 4B) suggested that the products resulting from the cleavage of KV-3 CPS with gp531 contain two linked glucose residues at the reducing end, as indicated by the spots corresponding to cellobiose, a disaccharide composed of two glucoses linked by a β-(1→4) glycosidic bond. Fig. 4B shows that glucose-containing disaccharide was gradually hydrolyzed by TFA to release glucose, resulting in an increase in the intensity of the spots corresponding to D-Glc*p*. Interestingly, while signals congruous with those of unreduced glucose were clearly visible in all samples containing CPS cleaved by gp531, spots for reduced glucose were not detected in the hydrolysates of reduced oligosaccharides. Moreover, Fig. 4 shows that neither fucose nor glucuronic acid could be detected in any of the analyzed samples while additional orange-colored spots could be seen in all the lanes showing TFA hydrolysates. This suggests that the acidic hydrolysis may have resulted in the formation of compounds of unknown structure, which subsequently interfered with the separation of samples during TLC analysis and complicated the interpretation of the results. Therefore, to clarify the sugar composition of the reduced oligosaccharide hydrolysates, the samples were also analyzed by HPLC-MS.

HPLC-MS analysis confirmed the presence of the glucose-containing disaccharide at the reducing end of the main products formed during the cleavage of KV-3 CPS with gp531. As shown in Fig. 5, during the acidic hydrolysis of gp531-generated oligosaccharides, a time-dependent decrease was observed in the signals corresponding to nonreduced (Fig. 5A) and reduced (Fig. 5C) cellobiose ions (365 *m/z* and 367 *m/z*, respectively). In contrast, the signals corresponding to nonreduced (Fig. 5B) and reduced (Fig. 5D) glucose ions (203 *m/z* and 205 *m/z*,
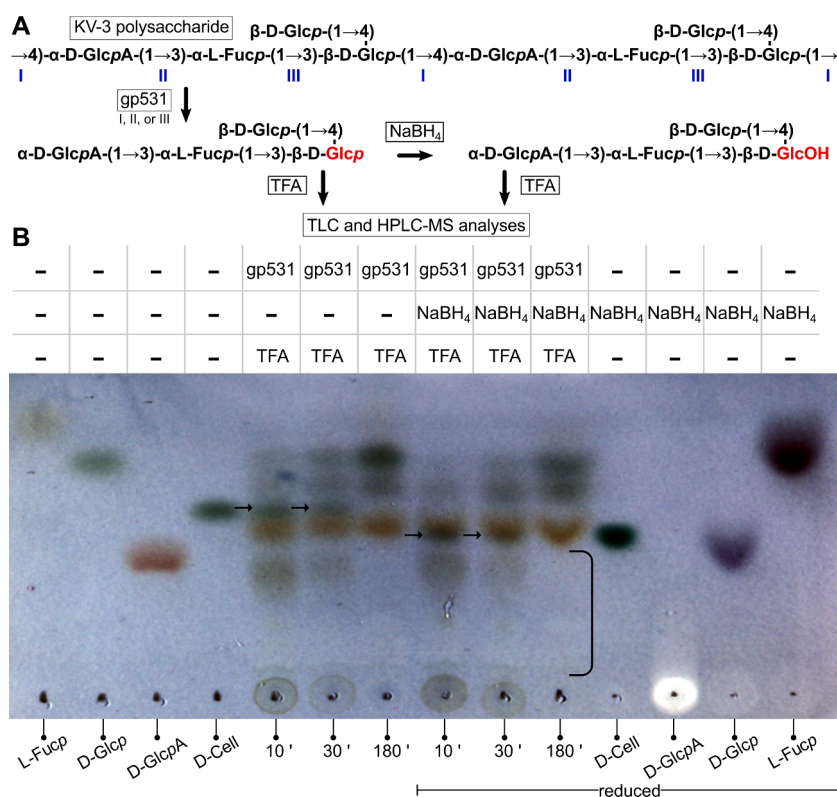

Fig. 4. TLC analysis of gp531-generated oligosaccharides reduced with NaBH₄ and hydrolyzed with TFA. (A) Scheme of the cleavage of CPS with gp531 and subsequent reduction and hydrolysis of the main reaction product. The glucose residue is highlighted in red, indicating its reduction into sorbitol (GlcOH). Note that for clarity, only one of the three possible tetrasaccharides is shown. (B) TLC analysis of oligosaccharides hydrolyzed with TFA. Commercial monosaccharides (both unreduced and reduced with NaBH₄) as well as unreduced products of KV-3 CPS depolymerization with gp531 were used as controls. The main constituents of the reaction mixtures are indicated at the top and bottom of the image. The duration of treatment with TFA is indicated at the bottom. Arrows indicate unreduced and reduced cellobiose, whereas partially hydrolyzed oligosaccharides are indicated by a bracket. The TLC mobile phase: 1-butOH: EtOH: dH₂O (5:3:2), and the total run time was 2 × 20 min.
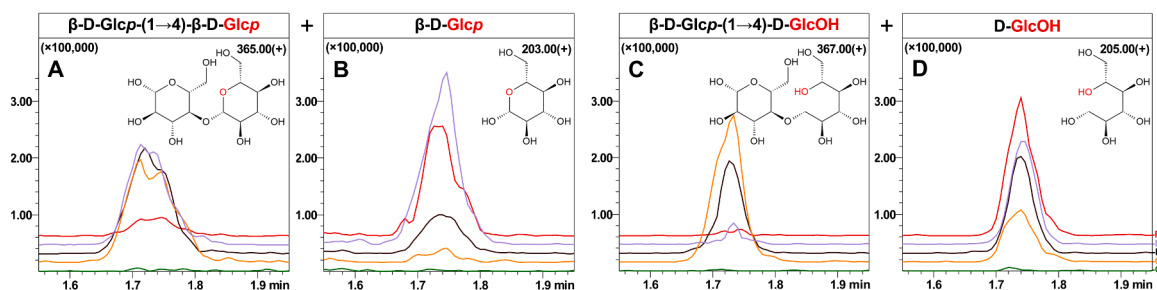
Fig. 5. HPLC-MS analysis of TFA hydrolysates obtained after the cleavage of *K. pneumoniae* KV-3 CPS with RaK2 gp531. Selected ion chromatograms representing: (A) cellobiose ([M+Na]$^+$, *m/z* 365), (B) glucose ([M+Na]$^+$, *m/z* 203), (C) reduced cellobiose ([M+Na]$^+$, *m/z* 367), and (D) reduced glucose ([M+Na]$^+$, *m/z* 205). The mass spectra obtained for commercial compounds, both NaBH$_4$-reduced and nonreduced, were used as a reference. The color code: green is TFA-untreated samples, whereas orange (10 min), black (30 min), purple (90 min), and red (180 min) are samples after hydrolysis with TFA. The HPLC gradient was 0.1 % HCOOH vs ACN.

respectively) exhibited an opposite trend, gradually increasing in intensity.

It is noteworthy that in TFA-untreated product samples, no signals corresponding to cellobiose or glucose (either reduced or nonreduced) were detected. Overall, both chromatography-based analyses indicated that the cleavage of KV-3 CPS with gp531 produces oligosaccharides with a glucose residue at the reducing end. However, due to the challenges in detecting reduced glucose monosaccharide in the TFA-treated product samples using TLC, and the difficulty in interpreting the HPLC-MS data due to the small 2-Da difference in molecular mass between reduced and unreduced compounds, an alternative approach was employed. In this second approach, we analyzed the structure of the tetrasaccharide, the main product of KV-3 CPS hydrolysis with gp531, derivatized with the ANTS fluorophore.

First, the total products of CPS hydrolysis were derivatized with ANTS. Then, the ANTS-tetrasaccharide was purified through ion-exchange chromatography followed by gel filtration, as illustrated in Fig. S2, and hydrolyzed with TFA. The resulting hydrolysis products were then analyzed by TLC (Fig. 6) using ANTS-derivatized saccharides as a control. The TLC analysis showed that after 10 min of acid hydrolysis, derivatized cellobiose and derivatized glucose were released from the ANTS-tetrasaccharide. As the hydrolysis time increased, ANTS-cellobiose was gradually cleaved while the amount of ANTS-glucose increased. Notably, spots seemingly corresponding to ANTS-fucose could be seen in the lanes showing ANTS-tetrasaccharide hydrolysates (Fig. 6A). However, since the migration profiles of ANTS itself and ANTS-derivatized fucose were nearly identical, these spots most likely corresponded to a free fluorophore rather than a derivatized sugar.
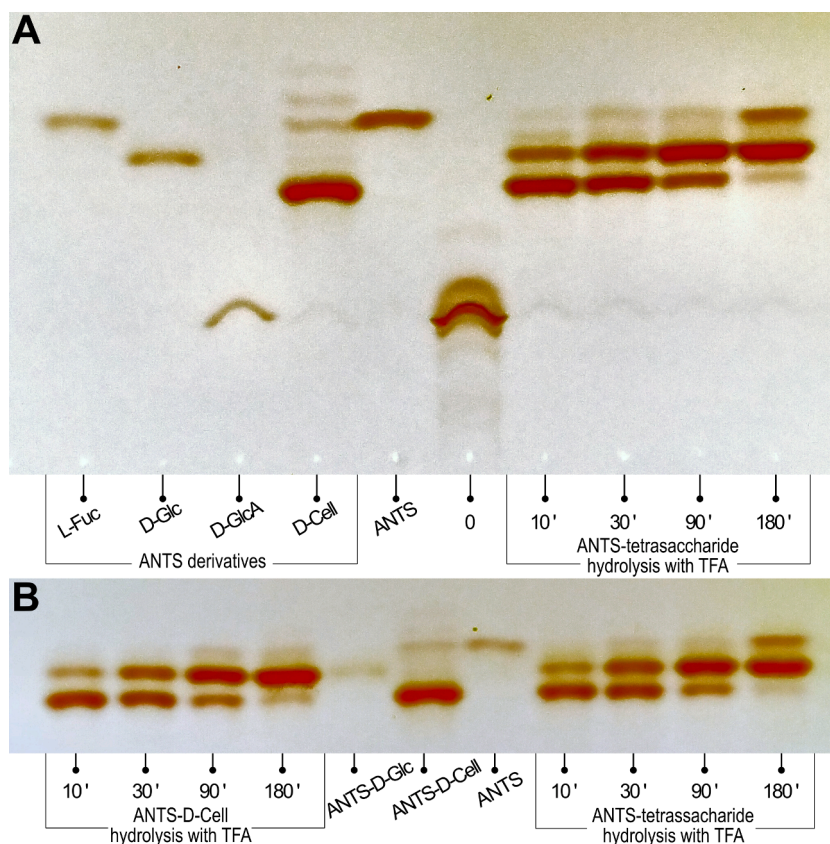

Fig. 6. TLC analysis of purified ANTS-derivatized product from gp531-catalyzed reaction (A, B), showing the samples taken before (0) and after 10–180-min TFA hydrolysis. TFA-treated ANTS-cellobiose as well as untreated ANTS-glucose, ANTS-fucose, ANTS-cellobiose, and ANTS were used as controls. The TLC mobile phase was 1-butOH: EtOH: dH$_2$O (5:3:2), and the total run time was 2 × 20 min.

The hydrolysates of ANTS-derivatized samples were subjected to HPLC-MS analysis as well. This analysis confirmed the findings from TLC, demonstrating that ANTS-glucose (m/z 548) is released from the derivatized tetrasaccharide during the acid hydrolysis (Fig. S3).

Taken together, the results obtained by both methods of modification of the reducing end clearly demonstrate that gp531 is a β-(1→4)-endo-glucosidase that specifically targets *Klebsiella* K54 CPS.

3.4. Evaluation of gp531 activity under different pH and temperature conditions

In the previous section, our main focus was on characterizing the enzymatic specificity of RaK2 gp531. Here, we aimed to investigate the effect of temperature and pH on the activity of gp531. To achieve this, we conducted depolymerization experiments using isolated *K. pneumoniae* KV-3 CPS and gp531, while varying the temperature from 10 to 70 °C and adjusting the pH of the buffer solutions from 3 to 10. The reaction products were analyzed using HPLC-MS to evaluate the relative activity of the enzyme. Specifically, the enzymatic activity of gp531 was quantified by integrating the total area of the ion peaks at m/z 663 and 687 within a 2–4 min range.

Fig. 7A shows that RaK2 gp531 exhibited consistently high enzymatic activity (92 ± 6 %) within the temperature range of 25–50 °C. However, over 50 °C, there was a rapid decrease in activity. As seen in Fig. 7B, gp531 is the most active in acidic solutions, with the optimum pH observed at 4.

In summary, investigation of RaK2 gp531 activity under different pH and temperature conditions revealed that the optimum temperature for an enzyme is 36 °C and the optimum pH is 4.

4. Discussion

Our previous study (Noreika et al., 2023) has provided valuable insights into the role of gp531 in the infection process of the jumbo bacteriophage RaK2. We have demonstrated that RaK2 gp531 functions as a tail fiber protein, which is an integral component of the phage's adsorption complex. We have shown that gp531 is essential for the successful attachment of the RaK2 virion particle to the host cell surface, as this protein, with its catalytic depolymerase domain, specifically recognizes and degrades the *K. pneumoniae* KV-3 capsule.

In the present study, we have identified this veterinary strain of *K. pneumoniae* as belonging to the K54 serotype by conducting a comparative analysis of the KV-3 *cps* gene cluster. Moreover, our investigation into the enzymatic activity of gp531 has confirmed this finding by showing that the main hydrolysis product of KV-3 CPS is a 664 Da tetrasaccharide, which corresponds to a repeating K-unit of K54. As mentioned in the introduction section, *K. pneumoniae* K54 belongs to a group of notorious medically relevant capsular variants (the others being K1, K2, K5, K20, and K57), most commonly found in hypervirulent strains of *K. pneumoniae* that are increasingly associated with life-threatening clinical conditions (Riwu et al., 2022; Taha et al., 2023; Wu et al., 2023). Moreover, Serotype K54 is distinguished by the rare presence of L-fucose residues, which is unusual for *Klebsiella* capsules, as only five other K-types (namely, K1, K6, K16, K58, and K63) have fucose as a structural unit of the CPS (Pan et al., 2015). It has been suggested that fucose-containing CPSs may enhance the ability of *Klebsiella* to evade phagocytosis (Wu et al., 2008; Kot et al., 2023). Interestingly, fucose-containing bacterial exopolysaccharides have recently been shown to have antioxidant, antimicrobial, anti-inflammatory, and even anticancer properties (Xiao et al., 2022).

We first started to explore the enzymatic specificity of gp531 depolymerase by providing the enzyme with a variety of substrates (e.g. commercial oligosaccharides, polysaccharides, and chromogenic carbohydrate or fatty acid derivatives). Our primary objective was to rapidly determine the catalytic range of gp531. However, gp531 did not cleave any of the 27 compounds tested. This result was not surprising given the generally high specificity of phage depolymerases. Since the active site of these normally trimeric enzymes is usually located in a large cleft formed by the neatly connected β-helices of each protein subunit, it specifically coordinates the polysaccharides and requires at least one repeating unit for optimal binding and catalysis (Dunstan et al., 2021; Tu et al., 2022).

During the hydrolysis of KV-3 CPS with gp531, the products obtained showed a range of sizes, with a major product consisting of a single repeating K-unit, indicating that gp531 is an endoglycosidase. This pattern of generating heterogeneous products comprising both single, double, and even triple repeating units, has also been observed in K57-targeting depolymerases from *Klebsiella* phages KpV79 and KpV767 (Volozhantsev et al., 2020). Interestingly, depolymerases encoded by phages infecting bacteria from genera other than *Klebsiella* (e.g., gp48 from *Acinetobacter baumannii* phage APK09) have been shown to cleave the bacterial CPS and do not release the monomer of the K-subunit, but only the dimer and trimer. In contrast, the cleavage of *A. baumannii* capsule K16 with depolymerase APK16_gp47 results only in monomeric K-units (Timoshina et al., 2023).

To identify the specific glycosidic bond targeted by RaK2 depolymerase, we modified the reducing end of the products released after hydrolysis of KV-3 CPS with gp531. TFA hydrolysis was then performed, and the product structure was analyzed by TLC and HPLC-MS. Although both methods had limitations, the two different approaches used in our study to modify the reducing end (reduction with NaBH$_4$ and derivatization by ANTS) led to the identification of the RaK2 depolymerase gp531 as a β-(1→4)-endoglucosidase. As discussed in the Introduction section, enzyme preparations from phage-infected bacteria played a valuable role in elucidating the structural properties of bacterial exopolysaccharides in studies conducted several decades ago (Dutton et al., 1981; Sutherland, 1972). One such study showed that, like RaK2 gp531, phage ø54-induced β-D-glucosidase cleaved the CPS of *Klebsiella* type K54 to yield tetra- and octasaccharides (Dell et al., 1983; Dutton and Merrifield, 1982). However, the genome sequence of phage ø54 and the
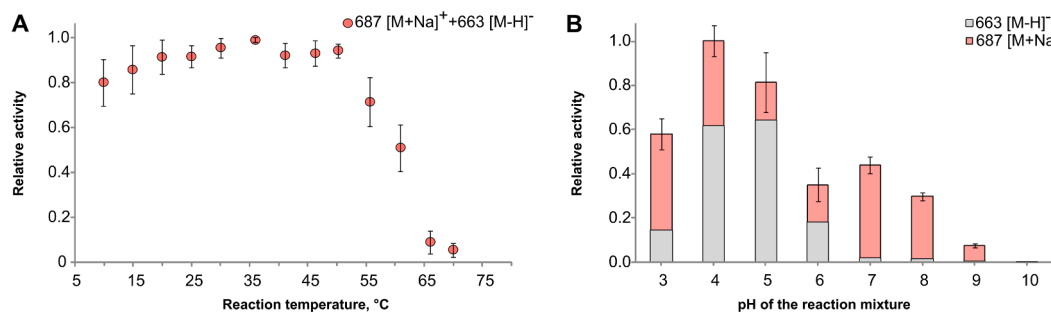

Fig. 7. Relative gp531 activity under different temperature (A) and pH (B) conditions. The data represent the total area of the ions of the main product of CPS hydrolysis with gp531 in negative and positive ionization modes. The values are presented as the mean ± standard deviation (SD) and were obtained from four independent replicates ($n = 4$).

proteins it encodes, including the potential depolymerase, remain unknown. Therefore, gp531 is currently the only characterized K54-specific β-(1→4)-endoglucosidase for which the amino acid sequence and the corresponding gene are published.

We also evaluated the enzymatic stability and optimal activity of gp531, which is crucial for utilizing the enzyme effectively in various biotechnological applications. We showed that gp531 exhibited prominent activity in acidic buffer solutions, with an optimum pH of 4 (overall pH range 3–8), and was highly active up to a temperature of 55 °C (optimum temperature 36 °C). In comparison, the K63-specific depolymerase DepoKP36 from *K. pneumoniae* phage KP36 retains activity within the pH range of 4–7, and temperatures up to 45 °C (Majkowska-Skrobek et al., 2016), while the K47-specific depolymerase Dep42 of *K. pneumoniae* phage SH-KP152226 is highly active in the pH range of 3.0 to 9.0 and at temperatures across 25 and 80 °C range (Wu et al., 2019). This suggests that *K. pneumoniae* phages, such as RaK2, are well-adapted to thrive in various ecological niches, including the gastrointestinal tract of warm-blooded animals.

Overall, the findings from this study provide important insights into the enzymatic properties of depolymerase gp531 encoded by the *K. pneumoniae* K54 jumbo phage RaK2. Continued research and exploration of gp531 and related enzymes are warranted to fully realize their potential in the development of novel therapeutic strategies, antimicrobial agents, or biotechnological applications targeting *K. pneumoniae*.

5. Conclusion

The depolymerase gp531 from the jumbo phage RaK2 specifically targets the capsule of *K. pneumoniae* K54, which contains rare L-fucose residues. Acting as a β-(1→4)-endoglucosidase, gp531 cleaves the K54 CPS within a pH range of 3 to 8 and at temperatures ranging from 10 to 60 °C. These characteristics position gp531 as a promising candidate for diverse applications in medicine, food, and the chemical industry.

CRediT authorship contribution statement

Algirdas Noreika: Conceptualization, Investigation, Data curation, Writing – original draft. **Jonita Stankevičiūtė:** Investigation, Data curation. **Rasa Rutkienė:** Investigation. **Rolandas Meškys:** Conceptualization, Data curation, Supervision. **Laura Kalinienė:** Writing – review & editing, Supervision, Project administration, Funding acquisition.

Declaration of Competing Interest

The authors declare that they have no known competing financial interests or personal relationships that could have appeared to influence the work reported in this paper.

Data availability

Klebsiella pneumoniae KV-3 (K54 serotype) whole-genome sequence data is stored at NCBI database with accession number, SAMN31360738.

All results and data obtained in this study are authentic and repeatable, and none of the material has been published or is under consideration elsewhere.

analysis.

Supplementary materials

Supplementary material associated with this article can be found, in the online version, at doi:10.1016/j.virusres.2023.199225.

References

Bales, P.M., Renke, E.M., May, S.L., Shen, Y., Nelson, D.C., 2013. Purification and characterization of biofilm-associated EPS exopolysaccharides from ESKAPE organisms and other pathogens. PLoS One 8, 1–8. https://doi.org/10.1371/journal.pone.0067950.

Bellich, B., Lagatolla, C., Rizzo, R., D'Andrea, M.M., Rossolini, G.M., Cescutti, P., 2020. Determination of the capsular polysaccharide structure of the *Klebsiella pneumoniae* ST512 representative strain KPB-1 and assignments of the glycosyltransferases functions. Int. J. Biol. Macromol. 155, 315–323. https://doi.org/10.1016/j.ijbiomac.2020.03.196.

Bellich, B., Ravenscroft, N., Rizzo, R., Lagatolla, C., D'Andrea, M.M., Rossolini, G.M., Cescutti, P., 2019. Structure of the capsular polysaccharide of the KPC-2-producing *Klebsiella pneumoniae* strain KK207-2 and assignment of the glycosyltransferases functions. Int. J. Biol. Macromol. 130, 536–544. https://doi.org/10.1016/j.ijbiomac.2019.02.128.

Bertozzi Silva, J., Storms, Z., Sauvageau, D., 2016. Host receptors for bacteriophage adsorption. FEMS Microbiol. Lett. 363, 1–11. https://doi.org/10.1093/femsle/fnw002.

Chen, Q., Wang, M., Han, M., Xu, L., Zhang, H., 2023. Molecular basis of *Klebsiella pneumoniae* colonization in host. Microb. Pathog. 177, 1–6. https://doi.org/10.1016/j.micpath.2023.106026.

Dell, A., Dutton, G.G., Jansson, P.E., Lindberg, B., Lindquist, U., Sutherland, I.W., 1983. Absence of O-formyl groups in *Klebsiella* polysaccharides. Carbohydr. Res. 122, 340–343. https://doi.org/10.1016/0008-6215(83)88346-3.

Dunstan, R.A., Bamert, R.S., Belousoff, M.J., Short, F.L., Barlow, C.K., Pickard, D.J., Wilksch, J.J., Schittenhelm, R.B., Strugnell, R.A., Dougan, G., Lithgow, T., 2021. Mechanistic insights into the capsule-targeting depolymerase from a *Klebsiella pneumoniae* bacteriophage. Microbiol. Spectr. 9 https://doi.org/10.1128/spectrum.01023-21.

Dutton, G.G., Di Fabio, J., Leek, D.M., Merrifield, E.H., Nunn, J.R., Stephen, A.M., 1981. Preparation of oligosaccharides vy the action of bacteriophage-brone enzymes on *Klebsiella* capsular polysaccharides. Carbohydr. Res. 97, 127–138. https://doi.org/10.1016/S0008-6215(00)80530-3.

Dutton, G.G., Merrifield, E.H., 1982. The capsular polysaccharide from *Klebsiella* serotype K54; location of the O-acyl groups, and a revised structure. Carbohydr. Res. 105, 189–203. https://doi.org/10.1016/S0008-6215(00)84967-8.

Dutton, G.G., Parolis, H., Joseleau, J.P., Marais, M.F., 1986. The use of bacteriophage depolymerization in the structural investigation of the capsular polysaccharide from *Klebsiella* serotype K3. Carbohydr. Res. 149, 411–423. https://doi.org/10.1016/S0008-6215(00)90061-2.

Effah, C.Y., Sun, T., Liu, S., Wu, Y., 2020. *Klebsiella pneumoniae*: an increasing threat to public health. Ann. Clin. Microbiol. Antimicrob. 19, 1–9. https://doi.org/10.1186/s12941-019-0343-8.

Fernandes, S., São-José, C., 2018. Enzymes and mechanisms employed by tailed bacteriophages to breach the bacterial cell barriers. Viruses 10, 1–22. https://doi.org/10.3390/v10080396.

Hager, F.F., Sützl, L., Stefanović, C., Blaukopf, M., Schäffer, C., 2019. Pyruvate substitutions on glycoconjugates. Int. J. Mol. Sci. 20, 1–37. https://doi.org/10.3390/ijms20194929.

Hsieh, P.F., Lin, H.H., Lin, T.L., Chen, Y.Y., Wang, J.T., 2017. Two T7-like bacteriophages, K5-2 and K5-4, each encodes two capsule depolymerases: isolation and functional characterization. Sci. Rep. 7, 1–13. https://doi.org/10.1038/s41598-017-04644-2.

Hsu, C., Liao, C., Lin, T., Yang, H., Yang, F., 2016. Identification of a capsular variant and characterization of capsular acetylation in *Klebsiella pneumoniae* PLA-associated type. Nat. Publ. Gr. 1–13. https://doi.org/10.1038/srep31946.

Huynh, D.T.N., Kim, A.Y., Kim, Y.R., 2017. Identification of pathogenic factors in *Klebsiella pneumoniae* using impedimetric sensor equipped with biomimetic surfaces. Sensors 17, 1–13. https://doi.org/10.3390/s17061406.

Jongkees, S.A., Withers, S.G., 2014. Unusual enzymatic glycoside cleavage mechanisms. Acc. Chem. Res. 47, 226–235. https://doi.org/10.1021/ar4001313.

Knecht, L.E., Veljkovic, M., Fieseler, L., 2020. Diversity and function of phage encoded depolymerases. Front. Microbiol. 10, 1–16. https://doi.org/10.3389/fmicb.2019.02949.

Knirel, Y.A., Shneider, M.M., Popova, A.V., Kasimova, A.A., Senchenkova, S.N., Shashkov, A.S., Chizhov, A.O., 2020. Mechanisms of *Acinetobacter baumannii* capsular polysaccharide cleavage by phage depolymerases. Biochemistry 85, 567–574. https://doi.org/10.1134/S0006297920050053.

Knirel, Y.A., Van Calsteren, M.R., 2021. Bacterial exopolysaccharides. In: Barchi, J.J. (Ed.), Comprehensive Glycoscience, 2nd Edition. Elsevier Inc., Amsterdam, pp. 8–16. https://doi.org/10.1016/B978-0-12-819475-1.00005-5.

Kobata, A., 2013. Exo- and endoglycosidases revisited. Proc. Japan Acad. Ser. B Phys. Biol. Sci. 89, 97–117. https://doi.org/10.2183/pjab.89.97.

Kot, B., Piechota, M., Szweda, P., Mitrus, J., Wicha, J., Grużewska, A., Witeska, M., 2023. Virulence analysis and antibiotic resistance of *Klebsiella pneumoniae* isolates from

hospitalised patients in Poland. Sci. Rep. 13, 1–12. https://doi.org/10.1038/s41598-023-31086-w.

Li, P., Ma, W., Shen, J., Zhou, X., 2022. Characterization of novel bacteriophage vB _ KpnP _ ZX1 and its depolymerases with therapeutic potential for K57 *Klebsiella pneumoniae* infection. Pharmaceutics 14, 1–20. https://doi.org/10.3390/pharmaceutics14091916.

Lin, T.L., Hsieh, P.F., Huang, Y.T., Lee, W.C., Tsai, Y.T., Su, P.A., Pan, Y.J., Hsu, C.R., Wu, M.C., Wang, J.T., 2014. Isolation of a bacteriophage and its depolymerase specific for K1 capsule of *Klebsiella pneumoniae*: implication in typing and treatment. J. Infect. Dis. 210, 1734–1744. https://doi.org/10.1093/infdis/jiu332.

Majkowska-Skrobek, G., Łątka, A., Berisio, R., Maciejewska, B., Squeglia, F., Romano, M., Lavigne, R., Struve, C., Drulis-Kawa, Z., 2016. Capsule-targeting depolymerase, derived from *Klebsiella* KP36 phage, as a tool for the development of anti-virulent strategy. Viruses 8, 1–7. https://doi.org/10.3390/v8120324.

Majkowska-Skrobek, G., Latka, A., Berisio, R., Squeglia, F., Maciejewska, B., Briers, Y., Drulis-Kawa, Z., 2018. Phage-borne depolymerases decrease *Klebsiella pneumoniae* resistance to innate defense mechanisms. Front. Microbiol. 9, 1–12. https://doi.org/10.3389/fmicb.2018.02517.

Navon-Venezia, S., Kondratyeva, K., Carattoli, A., 2017. *Klebsiella pneumoniae*: a major worldwide source and shuttle for antibiotic resistance. FEMS Microbiol. Rev. 41, 252–275. https://doi.org/10.1093/femsre/fux013.

Niemann, H., Frank, N., Stirm, S., 1977. *Klebsiella* serotype-13 capsular polysaccharide: primary structure and depolymerization by a bacteriophage-borne glycanase. Carbohydr. Res. 59, 165–177. https://doi.org/10.1016/S0008-6215(00)83303-0.

Noreika, A., Rutkiene, R., Dumalakienė, I., Vilienė, R., Laurynėnas, A., Povilonienė, S., Skapas, M., Meškys, R., Kaliniene, L., 2023. Insights into the alcyoneusvirus adsorption complex. Int. J. Mol. Sci. 24, 1–22. https://doi.org/10.3390/ijms24119320.

Olszak, T., Shneider, M.M., Latka, A., Maciejewska, B., Browning, C., Sycheva, L.V., Cornelissen, A., Danis-Wlodarczyk, K., Senchenkova, S.N., Shashkov, A.S., Gula, G., Arabski, M., Wasik, S., Miroshnikov, K.A., Lavigne, R., Leiman, P.G., Knirel, Y.A., Drulis-Kawa, Z., 2017. The O-specific polysaccharide lyase from the phage LKA1 tailspike reduces *Pseudomonas* virulence. Sci. Rep. 7, 1–14. https://doi.org/10.1038/s41598-017-16411-4.

Opoku-Temeng, C., Kobayashi, S.D., DeLeo, F.R., 2019. *Klebsiella pneumoniae* capsule polysaccharide as a target for therapeutics and vaccines. Comput. Struct. Biotechnol. J. 17, 1360–1366. https://doi.org/10.1016/j.csbj.2019.09.011.

Pan, S.Y., Litscher, G., Gao, S.H., Zhou, S.F., Yu, Z.L., Chen, H.Q., Zhang, S.F., Tang, M. K., Sun, J.N., Ko, K.M., 2014. Historical perspective of traditional indigenous medical practices: the current renaissance and conservation of herbal resources. Evidence-based Complement. Altern. Med. 2014, 1–20. https://doi.org/10.1155/2014/525340.

Pan, Y., Lin, T., Chen, C., Tsai, Y., Cheng, Y.H., Chen, Y.Y., Hsieh, P.F., Lin, Y.T., Wang, J. T., 2017. *Klebsiella* phage ΦK64-1 encodes multiple depolymerases for multiple host capsular types. ASM J. Virol. 91, 1–16. https://doi.org/10.1128/JVI.02457-16. PMCID: PMC5331798.

Pan, Y.J., Lin, T.L., Chen, C.T., Chen, Y.Y., Hsieh, P.F., Hsu, C.R., Wu, M.C., Wang, J.T., 2015. Genetic analysis of capsular polysaccharide synthesis gene clusters in 79 capsular types of *Klebsiella* spp. Sci. Rep. 5, 1–10. https://doi.org/10.1038/srep15573.

Parolis, H., Parolis, L.A., Whittaker, D.V., 1992. *Re*-investigation of the structure of the capsular polysaccharide of *Klebsiella* K15 using bacteriophage degradation and inverse-detected NMR experiments. Carbohydr. Res. 231, 93–103. https://doi.org/10.1016/0008-6215(92)84011-G.

Patro, L.P.P., Rathinavelan, T., 2019. Targeting the sugary armor of *Klebsiella* species. Front. Cell. Infect. Microbiol. 9, 1–23. https://doi.org/10.3389/fcimb.2019.00367.

Patro, L.P.P., Sudhakar, K.U., Rathinavelan, T., 2020. K-PAM: a unified platform to distinguish *Klebsiella* species K- and O-antigen types, model antigen structures and identify hypervirulent strains. Sci. Rep. 10, 1–15. https://doi.org/10.1038/s41598-020-73360-1.

Pertics, B.Z., Cox, A., Nyúl, A., Szamek, N., Kovács, T., Schneider, G., 2021. Isolation and characterization of a novel lytic bacteriophage against the K2 capsule-expressing hypervirulent *Klebsiella pneumoniae* strain 52145, and identification of its functional depolymerase. Microorganisms 9, 1–20. https://doi.org/10.3390/microorganisms9030650.

Podschun, R., Ullmann, U., 1998. *Klebsiella* spp. as nosocomial pathogens: epidemiology, taxonomy, typing methods, and pathogenicity factors. Clin. Microbiol. Rev. 11, 589–603. https://doi.org/10.1128/cmr.11.4.589.

Riwu, K.H.P., Effendi, M.H., Rantam, F.A., Khairullah, A.R., Widodo, A., 2022. A review: virulence factors of *Klebsiella pneumoniae* as emerging infection on the food chain. Vet. World 15, 2172–2179. https://doi.org/10.14202/vetworld.2022.2172-2179.

Rocha, J., Henriques, I., Gomila, M., Manaia, C.M., 2022. Common and distinctive genomic features of *Klebsiella pneumoniae* thriving in the natural environment or in clinical settings. Sci. Rep. 12, 1–10. https://doi.org/10.1038/s41598-022-14547-6.

Russo, T.A., Marr, C.M., 2019. Hypervirulent *Klebsiella pneumoniae*. Am. Soc. Microbiol. 32, 1–42. https://doi.org/10.1128/CMR.00001-19.

Shao, C., Xin, L., Mi, P., Jiang, M., Wu, H., 2022. Phenotypic and molecular characterization of K54-ST29 hypervirulent *Klebsiella pneumoniae* causing multi-system infection in a patient with diabetes. Front. Microbiol. 13, 1–9. https://doi.org/10.3389/fmicb.2022.872140.

Šimoliunas, E., Kaliniene, L., Truncaite, L., Zajančkauskaite, A., Staniulis, J., Kaupinis, A., Ger, M., Valius, M., Meškys, R., 2013. *Klebsiella* phage vB_KleM-RaK2 - a giant singleton virus of the family Myoviridae. PLoS One 8, 1–11. https://doi.org/10.1371/journal.pone.0060717.

Squeglia, F., Maciejewska, B., Łątka, A., Ruggiero, A., Briers, Y., Drulis-Kawa, Z., Berisio, R., 2020. Structural and functional studies of a *Klebsiella* phage capsule depolymerase tailspike: mechanistic insights into capsular degradation. Structure 28, 613–624. https://doi.org/10.1016/j.str.2020.04.015.

Stone, B.A., Svensson, B., Collins, M.E., Rastall, R.A., 2008. Polysaccharide degradation. In: Fraser-Reid, B.O., Tatsuta, K., Thiem, J. (Eds.), Glycoscience. Springer, Berlin, Heidelberg, pp. 2325–2375. https://doi.org/10.1007/978-3-540-30429-6_60.

Sutherland, I.W., 1972. Bacterial exopolysaccharides. Adv. Microb. Physiol. 8, 143–213. https://doi.org/10.1016/S0065-2911(08)60190-3.

Sutherland, I.W., 1971. The exopolysaccharides of *Klebsiella* serotype 2 strains as substrates for phage-induced polysaccharide depolymerases. J. Gen. Microbiol. 70, 331–338. https://doi.org/10.1099/00221287-70-2-331.

Sutherland, I.W., 1967. Phage-induced fucosidases hydrolysing the exopolysaccharide of *Klebsiella* arogenes type 54 [A3(S1)]. Biochem. J. 104, 278–285. https://doi.org/10.1042/bj1040278.

Sutherland, I.W., Wilkinson, J., 1968. The exopolysaccharide of *Klebsiella aerogenes* A3 (SI) (Type 54). Biochem. J. 4, 749–754. https://doi.org/10.1042/bj1100749.

Taha, M.S., Hagras, M.M., Shalaby, M.M., Zamzam, Y.A., Elkolaly, R.M., Abdelwahab, M. A., Maxwell, S.Y., 2023. Genotypic characterization of carbapenem-resistant *Klebsiella pneumoniae* Isolated from an Egyptian University Hospital. Pathogens 12, 1–14. https://doi.org/10.3390/pathogens12010121.

Thurow, H., Niemann, H., Rudolph, C., Stirm, S., 1974. Host capsule depolymerase activity of bacteriophage particles active on *Klebsiella* K20 and K24 strains. Virology 58, 306–309. https://doi.org/10.1016/0042-6822(74)90166-4.

Timoshina, O.Y., Kasimova, A.A., Shneider, M.M., Matyuta, I.O., Nikolaeva, A.Y., Evseev, P.V., Arbatsky, N.P., Shashkov, A.S., Chizhov, A.O., Shelenkov, A.A., Mikhaylova, Y.V., Slukin, P.V., Volozhantsev, N.V., Boyko, K.M., Knirel, Y.A., Miroshnikov, K.A., Popova, A.V., 2023. Friunavirus phage-encoded depolymerases specific to different capsular types of *Acinetobacter baumannii*. Int. J. Mol. Sci. 24, 1–25. https://doi.org/10.3390/ijms24109100.

Tu, I.F., Lin, T.L., Yang, F.L., Lee, I.M., Tu, W.L., Liao, J.H., Ko, T.P., Wu, W.J., Jan, J.T., Ho, M.R., Chou, C.Y., Wang, A.H.J., Wu, C.Y., Wang, J.T., Huang, K.F., Wu, S.H., 2022. Structural and biological insights into *Klebsiella pneumoniae* surface polysaccharide degradation by a bacteriophage K1 lyase: implications for clinical use. J. Biomed. Sci. 29, 1–17. https://doi.org/10.1186/s12929-022-00792-4.

Ucieklak, K., Koj, S., Pawelczyk, D., Niedziela, T., 2017. Structural masquerade of plesiomonas shigelloides strain CNCTC 78/89 O-antigen—High-resolution magic angle spinning nmr reveals the modified D-galactan I of *Klebsiella pneumoniae*. Int. J. Mol. Sci. 18, 1–20. https://doi.org/10.3390/ijms18122572.

Volozhantsev, N.V., Shpirt, A.M., Borzilov, A.I., Komisarova, E.V., Krasilnikova, V.M., Shashkov, A.S., Verevkin, V.V., Knirel, Y.A., 2020. Characterization and therapeutic potential of bacteriophage-encoded polysaccharide depolymerases with β galactosidase activity against *Klebsiella pneumoniae* K57 capsular type. Antibiotics 9, 1–16. https://doi.org/10.3390/antibiotics9110732.

Venturini, C., Ben Zakour, N.L., Bowring, B., Morales, S., Cole, R., Kovach, Z., Branston, S., Kettle, E., Thomson, N., Iredell, J.R., 2020. Fine capsule variation affects bacteriophage susceptibility in *Klebsiella pneumoniae* ST258. FASEB J. 34, 10801–10817. https://doi.org/10.1096/fj.201902735R.

Wang, C., Li, P., Niu, W., Yuan, X., Liu, H., Huang, Y., An, X., Fan, H., Zhangxiang, L., Mi, L., Zheng, J., Liu, Y., Tong, Y., Mi, Z., Bai, C., 2019. Protective and therapeutic application of the depolymerase derived from a novel KN1 genotype of *Klebsiella pneumoniae* bacteriophage in mice. Res. Microbiol. 170, 156–164. https://doi.org/10.1016/j.resmic.2019.01.003.

Wick, R.R., Heinz, E., Holt, K.E., Wyres, K.L., 2018. Kaptive web: user-Friendly capsule and lipopolysaccharide serotype prediction for *Klebsiella* genomes. J. Clin. Microbiol. 56, 1–10. https://doi.org/10.1128/JCM.00197-18.

Wilson, M., 2002. Bacterial Adhesion to Host Tissues: Mechanisms and Consequences, Bacterial Adhesion to Host Tissues. Cambridge University Press. https://doi.org/10.1017/cbo9780511541575.

Wu, J.H., Wu, A.M., Tsai, C.G., Chang, X.Y., Tsai, S.F., Wu, T.S., 2008. Contribution of fucose-containing capsules in *Klebsiella pneumoniae* to bacterial virulence in mice. Exp. Biol. Med. 233, 64–70. https://doi.org/10.3181/0706-RM-170.

Wu, J.W., Wang, J.T., Lin, T.L., Liu, Y.Z., Wu, L.T., Pan, Y.J., 2023. Identification of three capsule depolymerases in a bacteriophage infecting *Klebsiella pneumoniae* capsular types K7, K20, and K27 and therapeutic application. J. Biomed. Sci. 30, 1–12. https://doi.org/10.1186/s12929-023-00928-0.

Wu, Y., Wang, R., Xu, M., Liu, Y., Zhu, X., Qiu, J., Liu, Q., He, P., Li, Q., 2019. A novel polysaccharide depolymerase encoded by the phage SH-KP152226 confers specific activity against multidrug-resistant *Klebsiella pneumoniae* via biofilm degradation. Front. Microbiol. 10, 1–15. https://doi.org/10.3389/fmicb.2019.02768.

Xiao, M., Ren, X., Yu, Y., Gao, W., Zhu, C., Sun, H., Kong, Q., Fu, X., Mou, H., 2022. Fucose-containing bacterial exopolysaccharides: sources, biological activities, and food applications. Food Chem. X 13, 100233. https://doi.org/10.1016/j.fochx.2022.100233.

Zamze, S., Martinez-Pomares, L., Jones, H., Taylor, P.R., Stillion, R.J., Gordon, S., Wong, S.Y.C., 2002. Recognition of bacterial capsular polysaccharides and lipopolysaccharides by the macrophage mannose receptor. J. Biol. Chem. 277, 41613–41623. https://doi.org/10.1074/jbc.M207057200.

Zhu, J., Wang, T., Chen, L., Du, H., 2021. Virulence Factors in Hypervirulent *Klebsiella pneumoniae*. Front. Microbiol. 12, 1–14. https://doi.org/10.3389/fmicb.2021.642484.